COMPUTER METHODS IN MATERIALS SCIENCE

2025, vol. 25, no. 3, 35–46
https://doi.org/10.7494/cmms.2025.3.1022

Analysis of the decay time and bound-states energies of a particle in a specific structure GaMnAs/GaAs quantum well

Alaa Y. Ali[1,2*], Hassan H. Ali[3], Mustafa Y. Ali[1]

[1] Electrical Department, Engineering College Alshirqat, Tikrit University, Iraq.
[2] Natural Resources Research Center, Tikrit University, Iraq.
[3] Physics Department, College of Education for Pure Science, Tikrit University, Iraq.

Abstract

The bound states and decay time in a certain quantum well structure (GaMnAs/GaAs) were analysed and identified at the minimum decay time. Through the analysis of quantum mathematical equations, we derived specific formulas for energies that significantly amplify the numerical solutions of equations throughout all dimensions of confinement. Without altering the parameters utilized, the quantification, barriers, and well width were predominantly influenced by the spatial dimension parameters, such as the barrier height and well width. The principal bound state and lowest decay time were determined at a well width of 40 Å and a barrier thickness of 46.27 Å. This work revealed a novel characteristic known as interfacial tunnelling, which refers to the phenomenon where an electron establishes a tunnelling state between two interfaces. This tunnelling process is significantly influenced by the characteristics of the materials used, as well as the dimensions of the wells and barriers.

Keywords: bound-states energy, GaMnAs/GaAs, quantum well, decay time

1. Introduction

Various mechanisms can influence bound state energy, including the medium barrier or potential height, particle-particle interaction, and strain field, upon which bound state energy is contingent (Brand & Hughes, 1987; Ejere et al., 2019). To enhance electron confinement beyond the geometric potential reduction and barrier height augmentation, various additional factors must be considered, including strain fields. Indirect transitions (IBT) may also occur via the bound state (CBS), which is initially diminished to 0.2 meV in semiconductor alloy systems due to lattice strain (Psarakis, 2005). The results unequivocally demonstrate that CBS can generate stress that is several orders of magnitude greater than ABS (Ariyawansa et al., 2005; Oglah et al., 2021). This indicates that the quantum well (QW) containing CBS exhibits the most significant temperature dependence in electronic transport behaviour (Ohya, 2010; Rodrigues et al., 2012). To comprehend the bound state energy characteristics of III-V-based ferromagnetic semiconductor heterostructures, it is essential to investigate the parameters of the GaMnAs quantum well. This will enable us to obtain a deeper comprehension of the bound states and their impact on electronic transport. This will aid in the creation of devices with enhanced performance and increased efficiency.

* Corresponding author
Author's e-mails: alaa.y.ali@tu.edu.iq, hassan.h.ali@tu.edu.iq, mustafaali@tu.edu.iq
ORCID ID's: 0000-0002-7095-2328 (A. Y. Ali), 0009-0000-9718-4907 (H. H. Ali), 0009-0002-9671-3250 (M. Y. Ali)
Received: 30.05.2025, accepted: 15.09.2025, published: 4.12.2025

To achieve this end, we will derive precise solutions for the independent Schrödinger equation, taking into account various potential functions, including single square wells, double square wells, periodic square wells, and harmonic periodic wells. We employ an effective numerical technique known as the finite difference method (FDM), in conjunction with a combination of symmetric and asymmetric boundary conditions, to derive precise numerical solutions for various potential functions (Bastard & Brum, 1986; Hutchings, 1989).

The limited-area wave equation is utilised in spatial discretisation. Upon computing all elements of the potential function, the wave equation was resolved to derive several solutions. The answers were investigated further to determine the bound state energies and their associated wave functions.

The finite difference analysis of the Schrödinger equation (Anemogiannis et al., 1993; Oglah, 2024) yields precise determinations of bound state energy and wave functions for various potential functions. The results obtained can be used to examine the behaviour of electrons and the structural characteristics of materials, including ferromagnetic semiconductors, quantum wells, and nanostructures. This method can also elucidate the role of carriers or electron levels in these materials and their interactions with other energy states, providing insight into the materials' behaviour.

A potential well with magnetic barriers modifies the wavefunction at the edges by altering the energy spectrum and potentially leading to wave-vector filtering or Fabry–Pérot oscillations. The magnetic barriers can confine charge carriers, especially in materials like graphene nanoribbons, and affect the transmission and conductance through the structure (Xu et al., 2008).

The decay time in quantum wells refers to the time it takes for the excited state of a trapped electron-hole pair (exciton) to return to its ground state, often accompanied by the emission of light (photoluminescence). This decay can occur through radiative (light emission) or non-radiative (heat transfer or other forms of energy) processes.

Utilising the independent Schrödinger equation to simulate the behaviour of wave functions and their eigenvalues in bound states is a widely used method for understanding quantum systems. Solving the Schrödinger equation, either numerically or analytically, yields information regarding the energy levels, wave functions, and decay characteristics of the system. This work aims to solve the independent Schrödinger equation for a variable potential function $V(x)$, concentrating on the confinement condition of the carriers within a designated region of the well. In this scenario, the energy levels become quantised, necessitating the determination of the allowable energy values and their associated wave functions, as well as the minimum decay period. These solutions will possess significant real-world applications, including the vibration of molecules or electrons (Cortés et al., 2014).

2. Experimental procedure

In Hamiltonian and decay time, we can obtain additional information regarding the potential barriers by directing a beam of electrons at a specific angle, examining the transmission probability spectrum, and performing phase shift measurements. One objective of this analysis is to ascertain the bound states within these wells, along with their energies and probability distributions (Geltman, 2011).

Assessing the Hamiltonian influence of the system and the effective mass constitutes a fundamental aspect of the analysis. This entails the calculation of the kinetic and potential energy related to the elevation of potential barriers and their retention of magnetic impurities. We examine energies E that are less than the heights of the left and right potential barriers, $E < VL$ and $E < VR$. The states are correlated or concentrated within the potential barrier, indicating that the wave function in the regions adjacent to the barriers on the right and left aroaches zero (Chen, 1994; Oglah et al., 2020). The bound state produces a discrete energy lev referred to as the quantum mechanical bound state. It is a consequence of quantum confinement, a significant principle in quantum mechanics (Khan, 2011).

The decay period of the binding state in the quantum well can be determined using a two-level model, which characterises a system of E_1 and E_2 states confined by an identical potential. This model considers the energy levels of the two states as well as their connection. The coupling can be determined from the cross-integration of the wave functions of the two states. The decay rate can be determined via the exponential decay formula (Koç & Haydargil, 2004).

The particle's mobility is confined to region II, where $E < 0$; yet, it can ltrate the typically forbidden regions I or III. This indicates that the probability density is non-zero, and pursuant to the principle of indeterminacy, the particle may penetrate to a depth of Δx contingent upon its energy. It is observed that at least one bound state scenario must exist, as the movement of the classical energy body $E < 0$ is confined to zone II; nonetheless, this particle can infiltrate restricted regions according to traditions I and II, given that the probability density is not null. The depth attained by the particle is contingent upon its energy, as dictated by the principle of indeterminacy (Lucha & Schöberl, 1999).

For case of single well, Figure 1 represents the bound state energies in a single well, GaAs represents the quantum well, while GaMnAs represents the specific barrier material, as the height of the potential is 0.3 eV which represents the difference between GaAs, and GaMnAs, as we assume that the well width is L then we have (Ghatak, 1987; Istas et al., 2018):

$$V(x)=\begin{cases} V_0 & \text{in region I where} \quad x<0 \\ 0 & \text{in region II where} \quad 0<x<L \\ V_0 & \text{in region III where} \quad x>L \end{cases} \tag{1}$$

We will determine the wave function in the three regions, taking into account that it is terminated at the ends and continuous at the barriers at $x = 0$ and $x = L$.

$$\psi(x)=\begin{cases} Ae^{\alpha x} & \text{region I:} \quad x<0 \\ A\cos(\beta x)+B\sin(\beta x) & \text{region II:} \quad 0<x<L \\ [A\cos(\beta L)+B\sin(\beta L)]e^{-\alpha(x-L)} & \text{region III:} \quad L<x \end{cases} \tag{2}$$

whereas, A and B are optional constants as:

$$\beta=\frac{\sqrt{2mE}}{\hbar}, \quad \alpha=\frac{\sqrt{2m(V_0-E)}}{\hbar}$$

By applying boundary conditions at barriers and ends to the wave function, we have:

$$A\alpha - B\beta = 0$$

$$A(\alpha\cos(\beta L)-\beta\sin(\beta L))+B(\alpha\sin(\beta L)+\beta\cos(\beta L))=0 \tag{3}$$

$$\tan(\beta L)=\frac{2\beta\alpha}{\beta^2-\alpha^2} \tag{4}$$

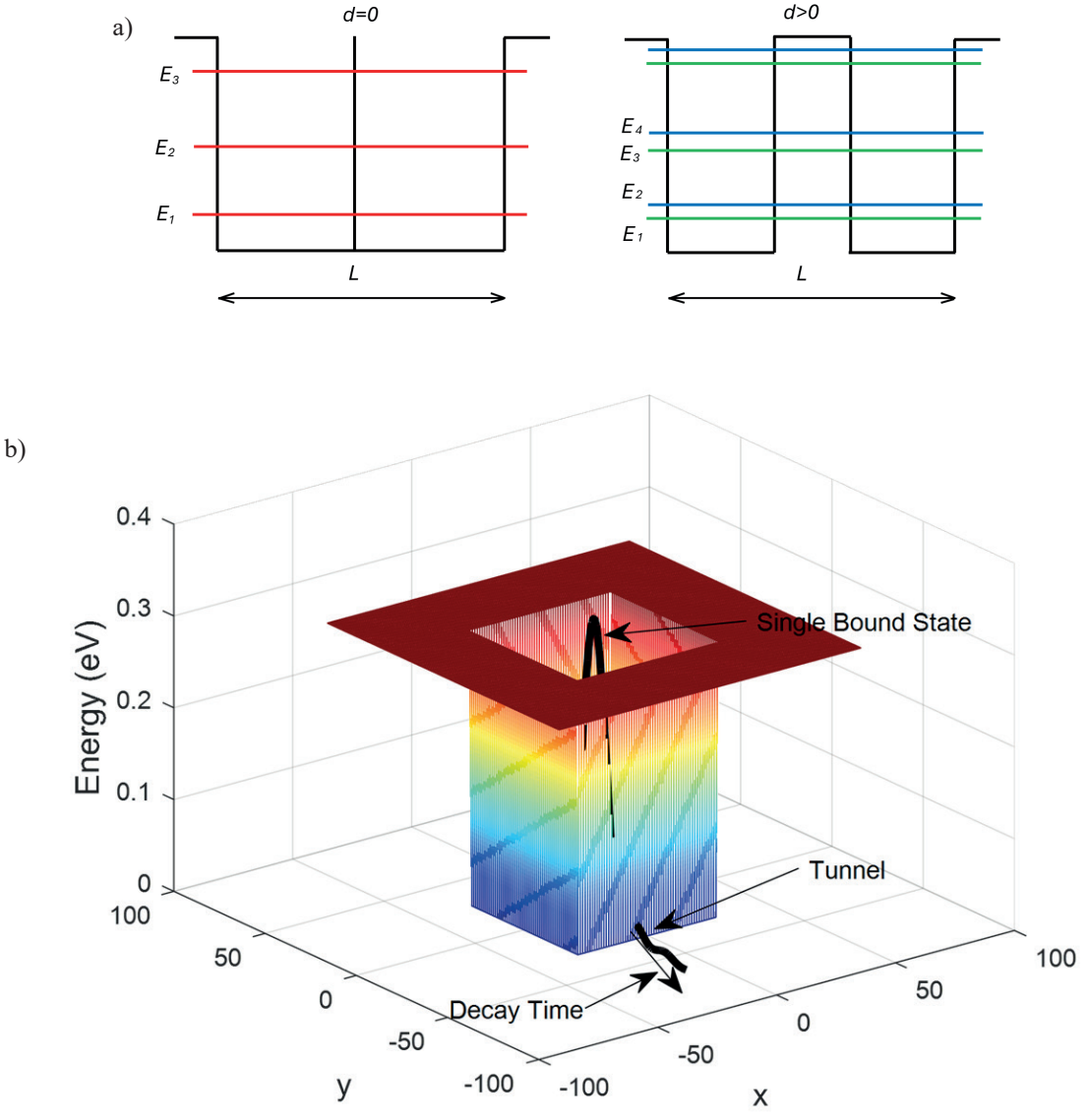

Fig. 1. The bound states of: a) the double-barrier well (for three cases of energy eigenvalue where they appear in the form of bound states); b) the single well (for one eigenvalue, including a visualisation of the tunnelling and gradient)

Now, solving Equation (4) gives the bound state energy, where once β and α have been determined, the thickness of the barrier d can be chosen so that the decay time is 1 Pa·s.

$$\tau = \frac{1}{\xi} = \frac{mL}{\hbar\beta} e^{2\alpha d} = 1 \text{ Pa} \cdot \text{s}, \text{ decay time is } \xi = \frac{\hbar\beta}{mL} e^{-2\alpha\beta}$$

The movement of the particles is limited to region II, where $E < 0$; however, this particle can penetrate the traditionally prohibited regions I or III. This means that the proba density is not equal to zero, and according to the principle of indeterminacy, the particle can penetrate to a depth of Δx depending on its energy. We note that there must be at least one bound state case as the movement of the classic energy body $E < 0$ is strictly limited to zone II; however, this particle can penetrate into forbidden areas by tradition I and II as the probability density is not equal to zero. The depth that the particle reaches can be determined depending on its energy through the principle of indeterminacy:

$$\Delta x \propto \frac{1}{k} = \frac{\hbar}{\sqrt{-2mE}} \to 0 \text{ for } |E| \to \infty$$

which will end in the barrier depth when the energy is large, accordingly, there is angular momentum created by the potential barrier:

$$\Delta p \propto \frac{\hbar}{k} = \sqrt{-2mE}$$

In the case of a double well, we will calculate the first two energies of the correlation state E_1 and E_2, then calculate the fluctuation period as follows (Bastard et al., 1984; Saha et al., 2007):

$$\tau = \frac{2\pi\hbar}{E_1 - E_2} \tag{5}$$

where $V(x) = 0.3$ eV.

$$(x) = \begin{cases} V_0, & x < -\dfrac{d}{2} - L \\ 0, & -\dfrac{d}{2} - L < x < -\dfrac{d}{2} \\ V_0, & -\dfrac{d}{2} < x < \dfrac{d}{2} \\ 0, & \dfrac{d}{2} < x < \dfrac{d}{2} + L \\ V_0, & \dfrac{d}{2} + L < x \end{cases} \tag{6}$$

$$\beta = \frac{\sqrt{2mE}}{\hbar}, \quad \alpha = \frac{\sqrt{2m(V_0 - E)}}{\hbar}$$

Given that the potential well is symmetric, therefore the wave function is either symmetric or asymmetric, and to obtain the symmetric wave function, we can follow the equation:

$$\psi(x) = \begin{cases} A\cosh(\alpha x) & 0 < x < \dfrac{d}{2} \\ B\sin(x) + C\cos(\beta x) & \dfrac{d}{2} < x < \dfrac{d}{2} + L \\ De^{-\alpha x} & \dfrac{d}{2} + L < x \end{cases} \tag{7}$$

The derivatives at the boundaries $x = d/2$, $x = d/2 + L$ are as follows:

$$\begin{bmatrix} \cosh\left(\dfrac{\alpha d}{2}\right) & -\sin\left(\dfrac{\beta d}{2}\right) & -\cos\left(\dfrac{\beta d}{2}\right) & 0 \\ \alpha A \sinh\left(\dfrac{\alpha d}{2}\right) & -\beta\cos\left(\dfrac{\beta d}{2}\right) & \beta\sin\left(\dfrac{\beta d}{2}\right) & 0 \\ 0 & \sin\left(\beta\left(\dfrac{d}{2} + L\right)\right) & \cos\left(\beta\left(\dfrac{d}{2} + L\right)\right) & -e^{-\alpha\left(\frac{d}{2}+L\right)} \\ 0 & \beta\cos\left(\beta\left(\dfrac{d}{2} + L\right)\right) & -\beta\sin\left(\beta\left(\dfrac{d}{2} + L\right)\right) & \end{bmatrix} \begin{bmatrix} A \\ B \\ C \\ D \end{bmatrix} = \begin{bmatrix} 0 \\ 0 \\ 0 \\ 0 \end{bmatrix} \tag{8}$$

To obtain non-zero solutions for constants A, B, C, and D, the determinants must be zero. This constrained solution gives us the bound state energies of similar solutions.

As for solutions to the asymmetric state, the wave function is:

$$\psi(x) = \begin{cases} A\sinh(\alpha x) & 0 < x < \dfrac{d}{2} \\ B\sin(\beta x) + C\cos(\beta x) & \dfrac{d}{2} < x < \dfrac{d}{2} + L \\ De^{-\alpha x} & \dfrac{d}{2} + L < x \end{cases} \tag{9}$$

The derivatives of the wave function at the boundaries are as follows:

$$\begin{bmatrix} \sinh\left(\frac{\alpha d}{2}\right) & -\sin\left(\frac{\beta d}{2}\right) \\ \alpha A\cosh\left(\frac{\alpha d}{2}\right) & -\beta\cos\left(\frac{\beta d}{2}\right) \\ 0 & \sin\left(\beta\left(\frac{d}{2}+L\right)\right) \\ 0 & \beta\cos\left(\beta\left(\frac{d}{2}+L\right)\right) \end{bmatrix} \tag{10}$$

$$\begin{bmatrix} -\cos\left(\frac{\beta d}{2}\right) & 0 \\ \beta\sin\left(\frac{\beta d}{2}\right) & 0 \\ \cos\left(\beta\left(\frac{d}{2}+L\right)\right) & -e^{-\alpha\left(\frac{d}{2}+L\right)} \\ -\beta\sin\left(\beta\left(\frac{d}{2}+L\right)\right) & \alpha e^{-\alpha\left(\frac{d}{2}+L\right)} \end{bmatrix} \begin{bmatrix} A \\ B \\ C \\ D \end{bmatrix} = \begin{bmatrix} 0 \\ 0 \\ 0 \\ 0 \end{bmatrix}$$

The requirement that the matrix be equal to zero, as above, because they give bound state energies for asymmetric solutions, and since the state does not require dividing the solution into symmetric and asymmetric, we can only rely on constructing the wave function using eight parameters and equating its determinants to zero to get eight states of bound state energy. Accordingly:

$$\alpha\cot(\alpha L) + \beta = 0 \quad \text{for odd state} \tag{10a}$$

$$\alpha\tan(\alpha L) - \beta = 0 \quad \text{for even state} \tag{10b}$$

Which are called transcendental equations. These only have implicit solutions and can only be numerical or graphical solutions (Moiseyev, 2009).

3. Results and discussion

Solving Equations (10a, 10b) reveals that dissolution can be derived from either equation, as the waveform is characterized by two equations that illustrate a general relationship between the decay constant at the barriers and the wave vector at the quantum well, highlighting the challenge of establishing the boundary conditions for this general relationship. This pertains to the configuration of the interstitial structure.

Mathematically, there are no analytical techniques for determining the intersections of the two equations; therefore, it is essential to employ numerical approaches, whi may be limited and specialized. The graphic illustrates that the circular function can intersect each curve once at a designated value (n-th), with each intersection representing potential solutions that limit the periodicity of the function's tangent and cotangent within the defined range. The quantity of bound states is ascertained by dividing the calibrated wave vector by the branch width at the nth intersection, rounding to the nearest integer. The observable outcome indicates that there is invariably a minimum of one bound state within the well of the designated quantity, irrespective of the potential's influence or the well's width. This finding is illustrated by Figure 2, which demonstrate that the circle consistently intersects with the first branch of Equation (10a) at n_1, even when the radius is minimal, as the first branch invariably originates from the origin point.

a)

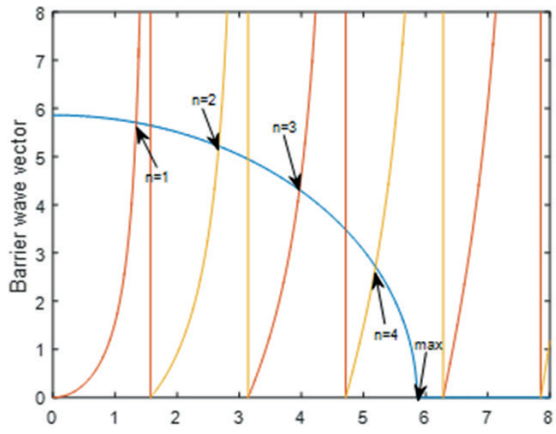

b)

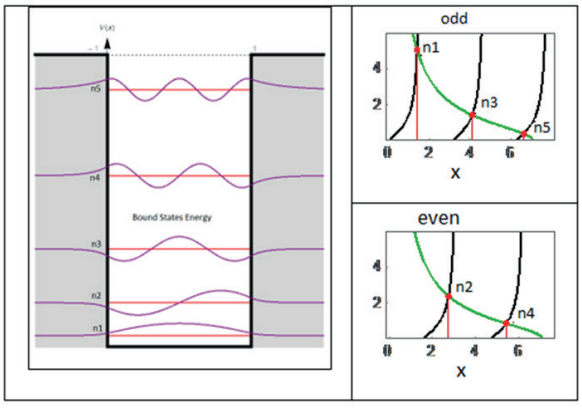

Fig. 2. A representation of conditions matching the bound state of a square GaAs well (a) and the bound states of a finite potential well (b) for Equations (10a, 10b). The GaAs well has a width of 100 Å and is surrounded by 300 MeV barriers. The left side of Equation (10a) is shown as a blue curve, while the right side is represented by curves in red; the wave vector intersections show the bound states. The maximum permissible value of the wave vector in the voltage well is V_{max}. The effective mass of an electron in the state of the GaAs well is 0.076 m

The width of the well influences the manifestation of bound states, however an increase in barrier thickness does not produce similar effects, as demonstrated in Figure 3. A distinct alteration in decay time relative to bound states occurs with an increase in quantum well width, as the number of bound states increases substantially with an extension in decay time (Fig. 4). Figure 4 indicates that the bound states increase with the well width is accompanied by an increase in decay time. This is unavailable in the event of a modification in the thickness of the barriers of the quantitative well of the GaMnAs/GaAs compound. Only two fixed values for bound states are shown, as illustrated in Figure 5.

The quantity of symmetric and asymmetric bound states or eigenfunctions escalates at energy levels E_1 and E_2, alongside an augmentation in decay time at well separations of 20 Å (Tab. 1) and 100 Å (Tab. 2), as illustrated in Figure 6, when the decay time commences its increase.

a)

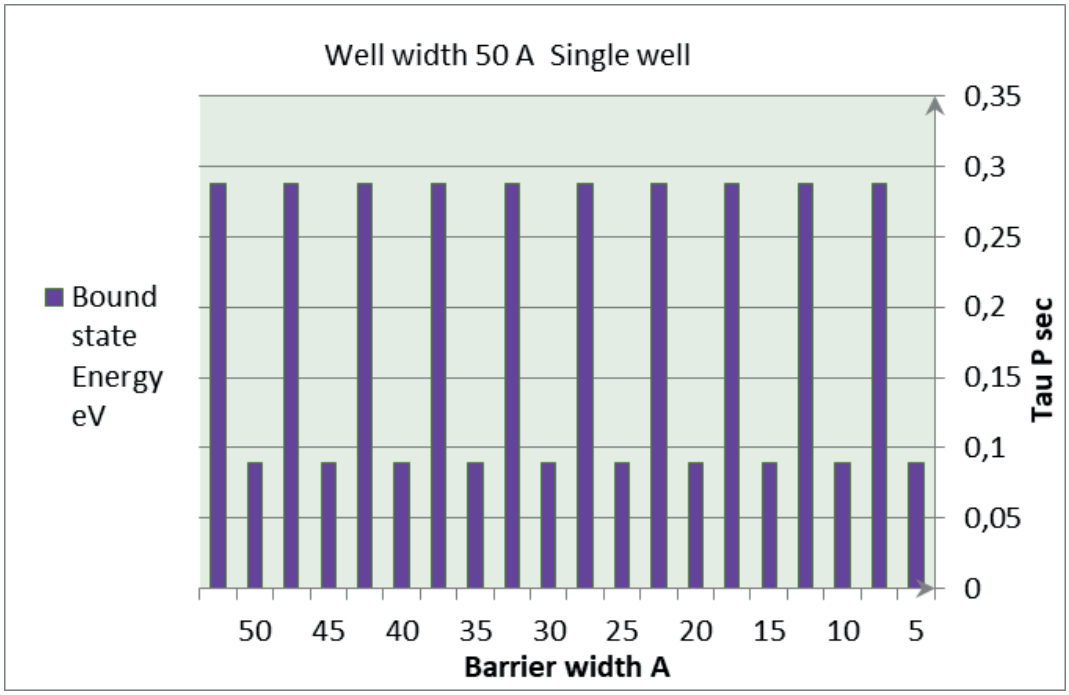

b)

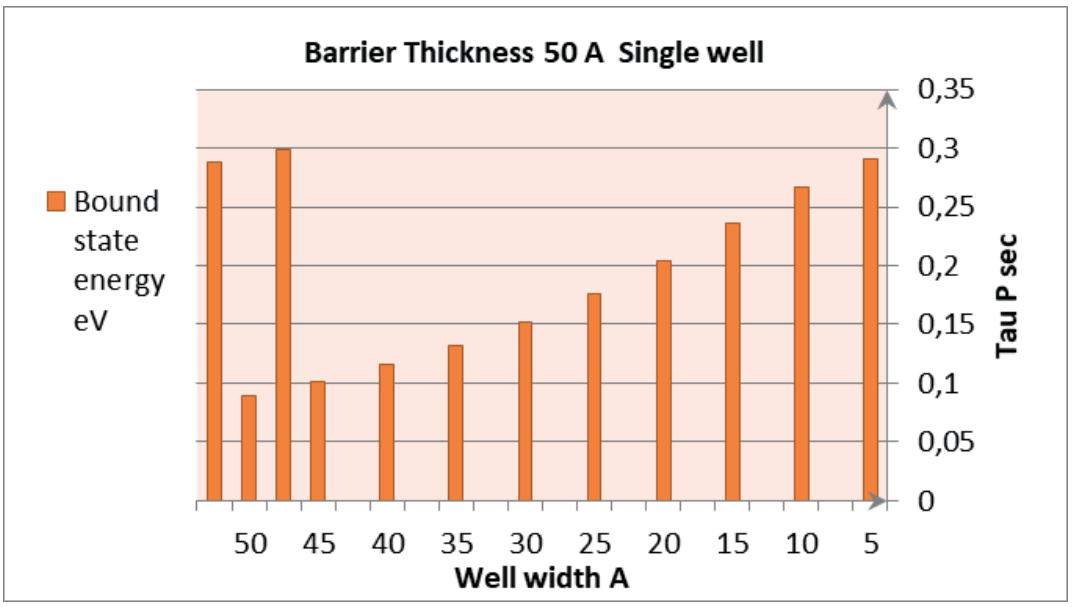

Fig. 3. Bound cases and the time of decay as a function of well width (a) and barrier thickness (b) at 50 Å. The bound cases are fixed and are not affected by the change in the thickness of the barriers. Figure b shows that there is an increase in the number of bound cases when the well width is accompanied by a noticeable increase in decay time, taking into account the barrier thickness at 50 Å

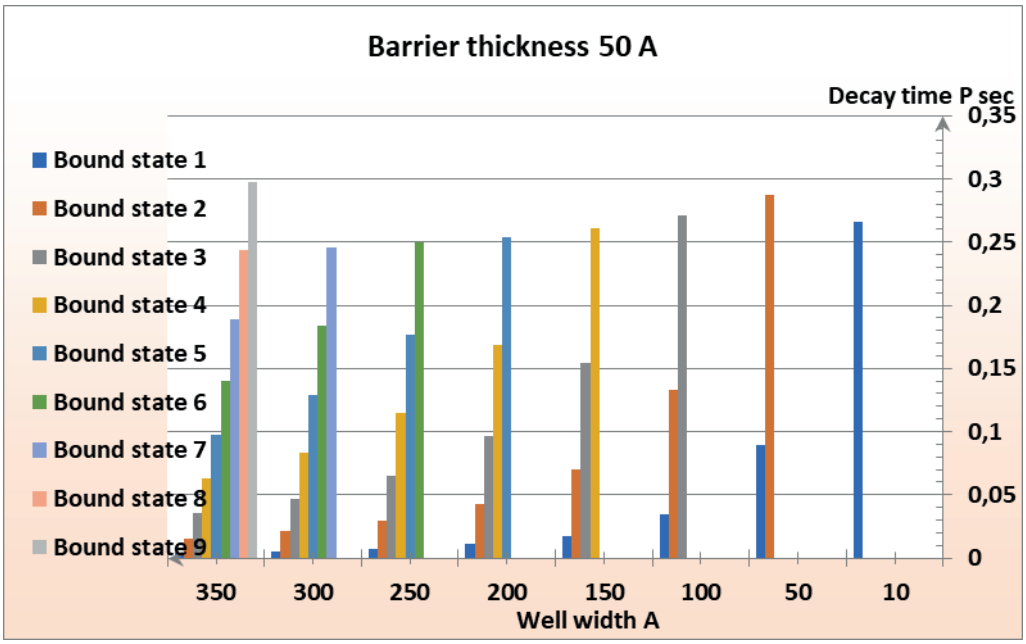

Fig. 4. The change in decay time and bound states with respect to the quantitative well width

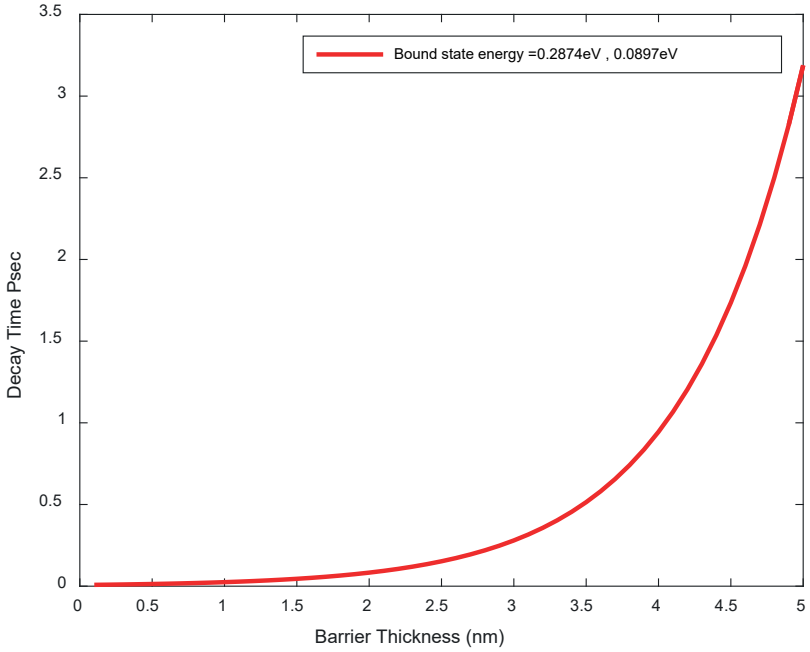

Fig. 5. The change of the decay time with the thickness of the barriers
(the depth of the well is 50 Å and the height of the barrier is 0.3 eV for the GaMnAs/GaAs compound).
Note that there are only two values for the bound state energy

Table 1. The bound state energy (BSE) and minimum decay time τ in seconds for a single quantum well

BSE [eV]	τ [s]
0.2	0.2
0.4	0.3
0.6	0.5
0.8	0.9

Table 2. The symmetrical and asymmetric states of the energy levels E_1 and E_2 with the decay time as a function of the quantum well width. Note that there is an increase in the number of symmetrical and asymmetric states with an increase in the decay at the well separations of about 20 Å

Well width [Å]	Decay time [P·s]	Symmetric solutions for bound state energy [eV]	Antisymmetric solutions for bound state energy [eV]
20	0.04830629	0.175350	0.260960
40	0.19727040	0.117230 0.278600	0.138200
60	0.78896840	0.076116 0.213710	0.289650 0.081358
80	2.5056	0.051482 0.168260 0.293020	0.053132 0.204360
100	6.5992	0.036694 0.130145 0.237920	0.037320 0.146380 0.299670
120	15.2201	0.027349 0.102680 0.197300	0.027620 0.109220 0.238200
140	31.9620	0.021127 0.081256 0.164910 0.255200	0.021256 0.084403 0.186720

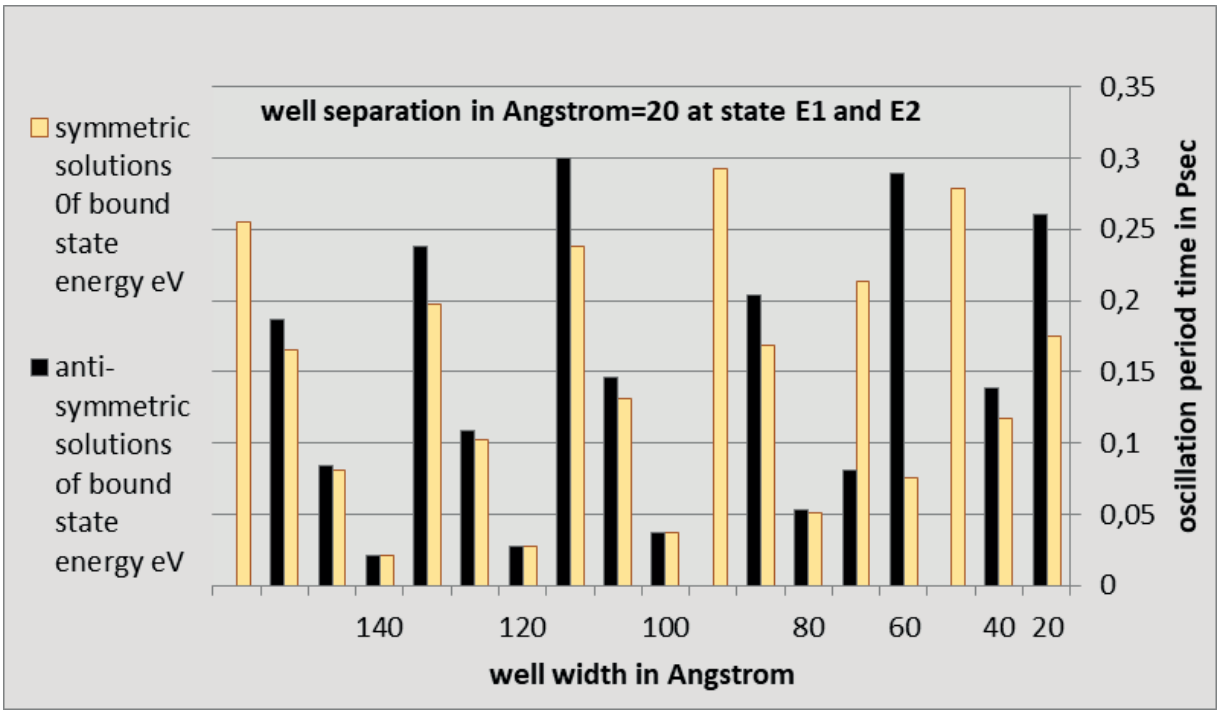

Fig. 6. The symmetrical and asymmetric states of the energy levels E_1 and E_2 with the time of decomposition as a function of the quantum well width. Note that there is an increase in the number of symmetrical and asymmetric states with an increase in the dissolution time at the well separations of about 20 Å

Figures 7 and 8 elucidate the variation of symmetric and asymmetric wave functions as a function of energy, given a well width of 100 Å and well separations of 20 Å at a designated decay time. Figure 8 shows that there is an increase in the number of symmetrical and asymmetric cases with a decrease in the decay time when increasing the intervals up to 100 Å, after which the decay time begins to increase.

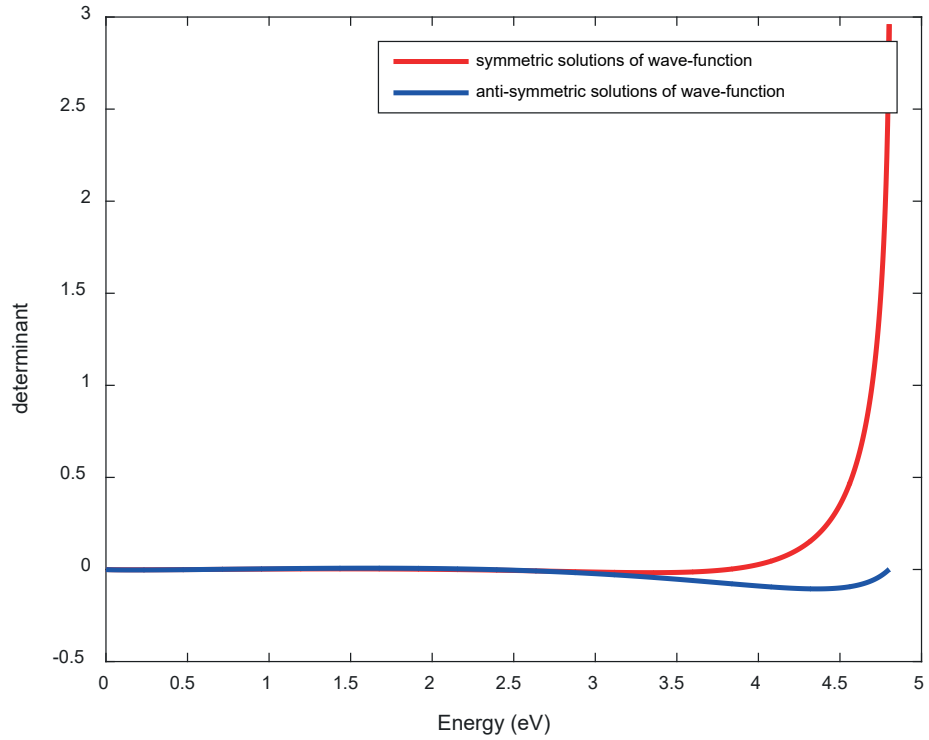

Fig. 7. The change of the symmetric and asymmetric wave functions as a function of energy when the well width is 100 Å and the well's separation is about 20 Å at a periodic time of 6.5992 picoseconds for the states E_1 and E_2

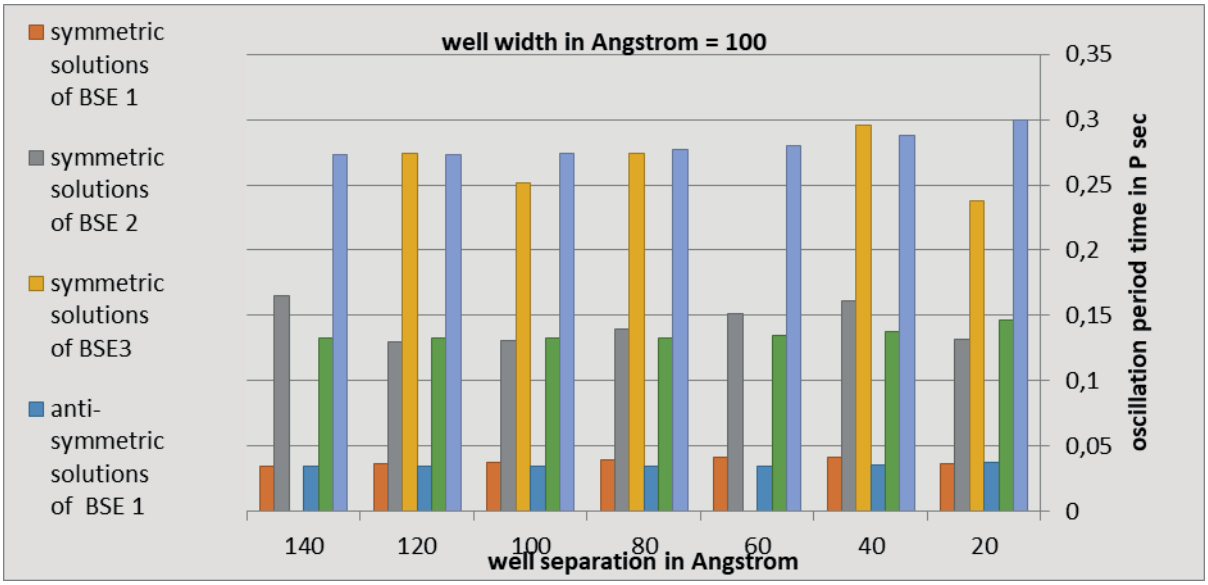

Fig. 8. The symmetrical and asymmetric bound states with the decay time, as a function of the quantum well separation

Table 3 also indicates that there is an increase in the number of symmetrical and asymmetric cases with a decrease in the decay time when increasing the separations up to 100 Å, after which the decay time begins to increase (Bohm, 2003).

Moreover, in this instance, it is necessary to adjust the decay time in relation to the well's width, as the energy of the bound state decreases with an increase in the well's width, while the decay time concurrently increases with the widening of the well.

This is contingent upon the stability of both the barrier thickness (50 Å) and the barrier height (0.3 eV) (Fig. 9). In this case, the decay time increases exponentially with increasing well width. The thickness of the barriers is 50 Å, and the height of the barriers is 0.3 eV.

Table 3. Asymmetric and asymmetric bound states with the decay time, as a function of the quantum well separations

Well separation [Å]	Decay time [Pa·s]	Symmetric solutions for bound state energy [eV]	Anti-symmetric solutions of bound state energy [eV]
20	6.5992	0.03669 0.13145 0.23792	0.03732 0.14638 0.29967
40	0.6295724	0.04164 0.16068 0.29563	0.03507 0.13726 0.28771
60	0.6079506	0.04123 0.15172	0.03443 0.13415 0.28046
80	0.7793651	0.03957 0.13965 0.27368	0.03426 0.13311 0.27666
100	1.1737	0.03774 0.13077 0.25126	0.03422 0.13276 0.27456
120	2.1653	0.03612 0.12941 0.27403	0.03421 0.13265 0.27336
140	6.3127	0.03486 0.16498	0.03420 0.13261 0.27265

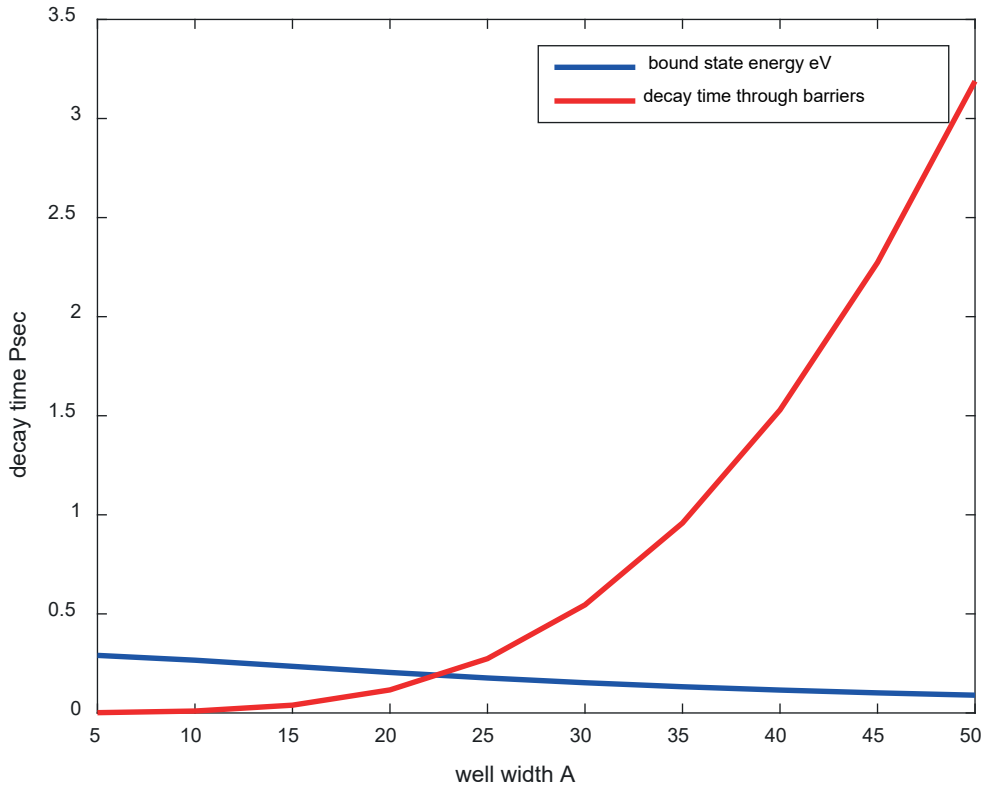

Fig. 9. The change in decay time with the width of the well, noting that the bound state energy decreases with increasing well width

4. Conclusion

The time-independent Schrödinger equation for symmetric and asymmetric wave functions in single and double potential wells was resolved by the application of suitable boundary conditions; bound states were derived from the energy eigenvalues, and the wave functions were determined from the variations in eigenvalues.

This type of well demonstrates that the upper states are bound states, while the lower states permit electron wave leakage. An analysis of the transport matrix corroborates the application of quantum wells in laser production, illustrating the influence of well width, thickness, and barrier height. These factors are also contingent upon the lifetime of the quasi-bound lower states, as the energy level may fluctuate with increasing barrier thickness, depending on the specific core point.

The bound states of single and double potential wells were analysed utilizing an appropriate transport matrix to address random well designs. The constrained cases were derived from both single and double quantitative wells, demonstrating robust hybridization for both heavy and light cases. This results in considerable reductions in the mass of the upper and lower valence, as the wave functions of the associated optical particles are localized at the interfaces, thereby correlating with the bonds and antigens at the edges of the quantum well. Currently, the separate interfaces facilitate the bound states that result in the generation of a light particle within the well, characterized by a significant amplitude of interference.

It was determined that bound state energy levels remain intact, as they are finite, yet they increase indefinitely depending on factors (α, β). Consequently, deeper potentials yield a greater number of bound states, and the spectrum of bound states exhibits even and odd alternations, with the ground state being equal. The decay time grows with the widening of the well and the thickening of the barriers, as bound states emerge with an increase in well width, while the height of the barriers remains unaffected.

The well width distinctly influences the cyclic decay period and the energy of both symmetric and asymmetric bound states of the wave function at the energy levels E_1 and E_2 in a double well system.

References

Anemogiannis, E., Glytsis, E. N., & Gaylord, T. K. (1993). Bound and quasi-bound state calculations for biased/unbiased semiconductor quantum heterostructures. *IEEE Journal of Quantum Electronics*, *29*(11), 2731–2740. https://doi.org/10.1109/3.248931

Ariyawansa, G., Perera, A. G. U., Raghavan, G. S., von Winckel, G., Stintz, A., & Krishna, S. (2005). Effect of well width on three-color quantum dots-in-a-well infrared detectors. *IEEE Photonics Technology Letters*, *17*(5), 1064–1066. https://doi.org/10.1109/LPT.2005.846753

Bastard, G., & Brum, J. (1986). Electronic states in semiconductor heterostructures. *IEEE Journal of Quantum Electronics*, *22*(9), 1625–1644. https://doi.org/10.1109/JQE.1986.1073186

Bastard, G., Ziemelis, U. O., Delalande, C., Voos, M., Gossard, A. C., & Wiegmann, W. (1984). Bound and virtual bound states in semiconductor quantum wells. *Solid State Communications*, *49*(7), 671–674. https://doi.org/10.1016/0038-1098(84)90218-7

Bohm, A. R. (2003). Time asymmetry and quantum theory of resonances and decay. *International Journal of Theoretical Physics*, *42*, 2317–2338. https://doi.org/10.1023/B:IJTP.0000005960.42318.f2

Brand, S., & Hughes, D. T. (1987). Calculations of bound states in the valence band of AlAs/GaAs/AlAs and AlGaAs/GaAs/AlGaAs quantum wells. *Semiconductor Science and Technology*, *2*(9), 607–614. https://doi.org/10.1088/0268-1242/2/9/007

Chen, J. J., Chan, A. K., & Chui, C. K. (1994). A local interpolatory cardinal spline method for the determination of eigenstates in quantum-well structures with arbitrary potential profiles. *IEEE Journal of Quantum Electronics*, *30*(2), 269–274. https://doi.org/10.1109/3.283769

Cortés, N., Chico, L., Pacheco, M., Rosales, L., & Orellana, P. A. (2014). Bound states in the continuum: Localization of Dirac-like fermions. *Europhysics Letters*, *108*(4). https://doi.org/10.1209/0295-5075/108/46008

Ejere, A. I., Okunzuwa, S., & Oloko, R. E. (2019). Analytical modeling for nanostructure quantum wells with equispaced energy levels in semiconductor ternary alloys (A_x B_{1-x} C). *Nigerian Journal of Technology (NIJOTECH)*, *38*(2), 437–443. https://doi.org/10.4314/NJT.V38I2.20

Geltman, S. (2011). Bound states in delta function potentials. *Journal of Atomic*, *Molecular and Optical Physics*, *2011*, 573179. https://doi.org/10.1155/2011/573179

Ghatak, A. K., Thyagarajan, K., & Shenoy, M. R. (1987). Numerical analysis of planar optical waveguides using matrix approach. *Journal of Lightwave Technology*, *LT-5*(5), 660–667. https://doi.org/10.1109/JLT.1987.1075553

Hutchings, D. C. (1989). Transfer matrix approach to the analysis of an arbitrary quantum well structure in an electric field. *Applied Physics Letters*, *55*(11), 1082–1084. https://doi.org/10.1063/1.101711

Istas, M., Groth, C., Akhmerov, A. R., Wimmer, M., & Waintal, X. (2018). A general algorithm for computing bound states in infinite tight-binding systems. *SciPost Physics*, *4*, 026. https://doi.org/10.21468/SciPostPhys.4.5.026

Khan, I. (2011). Analysis of a finite quantum well. *Journal of Electrical Engineering: The Institution of Engineers, Bangladesh*, *37*(2), 10–1.

Koç, R., & Haydargil, D. (2004). Solution of the Schrödinger equation with one- and two-dimensional double-well potentials. *Turkish Journal of Physics*, *28*, 161–167.

Lucha, W., & Schöberl, F. F. (1999). Solving the Schrödinger equation for bound states with Mathematica 3.0. *International Journal of Modern Physics C*, *10*(4), 607–619. https://doi.org/10.1142/S0129183199000450

Moiseyev, N. (2009). Suppression of Feshbach resonance widths in two-dimensional waveguides and quantum dots: A lower bound for the number of bound states in the continuum. *Physical Review Letters*, *102*, 167404. https://doi.org/10.1103/PhysRevLett.102.167404

Oglah, M. H. (2024). Analyzing the time evolution of a particle by decomposes the initial state confinement in 1D well into the lowest eigenstates energy. *Journal for Research in Applied Sciences and Biotechnology*, *3*(2), 103–107. https://doi.org/10.55544/jrasb.3.2.17

Oglah, M. H., Mohammed, S. J., & El-Daher, M. S. (2020). Determine the lower-state energy of (GaMn) As/GaAs quantum well using localization landscape method. *Tikrit Journal of Pure Science*, *25*(6), 96–102. https://doi.org/10.25130/tjps.v25i6.318

Oglah, M. H., Mohammed, S. J., & El-Daher, M. S. (2021). Simulation of energy resonant tunneling in short-period superlattice (Ga, Mn) As/GaAs quantum wells. *AIP Conference Proceedings*, *2372*(1), 040002. https://doi.org/10.1063/5.0065501

Ohya, S., Muneta, I., & Tanaka, M. (2010). Quantum-level control in III–V-based ferromagnetic-semiconductor heterostructure with a GaMnAs quantum well and double barriers. *Applied Physics Letters*, *96*(5), 052505. https://doi.org/10.1063/1.3298358

Psarakis, E. (2005). *Simulation of performance of quantum well infrared photodetectors* [Master's thesis, Naval Postgraduate School Monterey, California]. DTIC. https://apps.dtic.mil/sti/citations/ADA435542

Rodrigues, D. H., Brasil, M. J. S. P., Gobato, Y. G., Holgado, D. P. A., Marques, G. E., & Henini, M. (2012). Anomalous optical properties of GaMnAs/AlAs quantum wells grown by molecular beam epitaxy. *Journal of Physics D: Applied Physics*, *45*(21), 215301. https://doi.org/10.1088/0022-3727/45/21/215301

Saha, A., Bag, B. C., & Sarkar, P. (2007). Effects of barrier fluctuation on the tunneling dynamics in the presence of classical chaos in a mixed quantum-classical system. *Pramana: Journal of Physics*, *68*(3), 377–387. https://doi.org/10.1007/s12043-007-0041-5

Xu, H., Heinzel, T., Evaldsson, M., & Zozoulenko, I. V. (2008). Magnetic barriers in graphene nanoribbons: Theoretical study of transport properties. *Physical Review B: Condensed Matter and Materials Physics*, *77*(24), 245401. https://doi.org/10.1103/PhysRevB.77.245401